Journal of Colloid and Interface Science 468 (2016) 70–77

Contents lists available at ScienceDirect

Journal of Colloid and Interface Science

journal homepage: www.elsevier.com/locate/jcis

Fabrication of ordered honeycomb amphiphobic films with extremely low fluorine content

Fei Gao [a], Wei Wang [a], Xinxin Li [a,*], Lei Li [b], Jiaping Lin [a], Shaoliang Lin [a,*]

[a] Shanghai Key Laboratory of Advance Polymeric Materials, Key Laboratory for Ultrafine Materials of Ministry of Education, School of Materials Science and Engineering, East China University of Science and Technology, 200237 Shanghai, China
[b] College of Materials, Xiamen University, 361005 Xiamen, China

HIGHLIGHTS

- The honeycomb films of fluorinated copolymers are fabricated by breath figure technique.
- The influence of preparation conditions on the film surface features is investigated in details.
- Wetting behavior including hydrophobic property and wetting state of the films is explored.
- A facile approach to fabricate amphiphobic honeycomb film with extremely low fluorine content is presented.

GRAPHICAL ABSTRACT

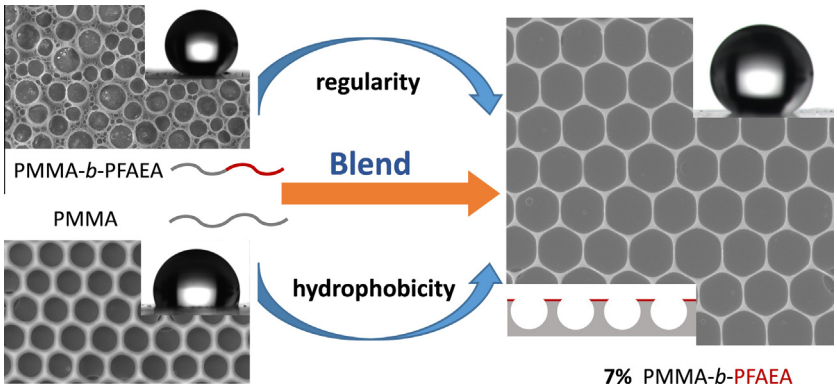

ARTICLE INFO

Article history:
Received 9 October 2015
Revised 15 January 2016
Accepted 18 January 2016
Available online 18 January 2016

Keywords:
Breath figure
Amphiphobic
Fluorinated polymer

ABSTRACT

A series of poly(methyl methacrylate)-*block*-poly(perfluoroalkyl ethyl acrylate) (PMMA-*b*-PFAEA) with various fluorine content were employed to fabricate honeycomb ordered films via breath figure strategy. The influences of temperature, concentration, relative humidity, fluorine content on the morphology of porous films were investigated. Wetting behavior including hydrophobic property and wetting state of the films was studied. High surface roughness from the porous structure and low surface free energy from the increasing PFAEA fraction led to the enhancement of hydrophobicity. Additionally, fabrication of porous films by the mixture of PMMA and PMMA-*b*-PFAEA was investigated. Ordered porous film with excellent hydrophobicity and oleophobicity was obtained with only 7 wt% of PMMA-*b*-PFAEA by simultaneous processes of breath figure mechanism and phase separation. This work facilitates our further comprehension of the mechanism of breath figure and contributes to the fabrication of porous film from fluorinated copolymers. Meanwhile, it opens a new route to prepare films possessing excellent hydrophobicity and oleophobicity with extremely low fluorine content.

1. Introduction

Ordered porous polymeric films have attracted a great deal of attention from the field of advanced material and have wide application prospects in catalyst supports [1,2], biological scaffolds [3–5], optical materials [6,7], filtering films [8,9], growing templates [10–12], and hydrophobic films [13,14] due to their competitive advantages including light weight, ordered alignment of pores, high specific surface area and great adsorption capacity [15–17]. Nevertheless, conventional methods to fabricate ordered porous films are mainly focused on direct writing, imprint and lithography

* Corresponding authors.
E-mail addresses: slin@ecust.edu.cn (S. Lin), xinxinli@ecust.edu.cn (X. Li).

http://dx.doi.org/10.1016/j.jcis.2016.01.035
0021-9797/

techniques, which have low throughput and need elaborate templates [18–21].

As a simple, versatile, template-free and economic technique, breath figure (BF) is a powerful tool for preparing films with highly ordered honeycomb structures and adjustable surface features [15]. The well-accepted forming mechanism of BF has been summarized and demonstrated by many researchers from the perspectives of experiments and simulations as the following process [22–24]. When polymer dissolved in organic solvent with low boiling point is cast on substrates under high humidity, rapid evaporative cooling results in the condensation of water vapor onto the solution surface. The water droplets grow with continuous condensation, stabilized by instant precipitation of polymer, and self-assemble into ordered droplet arrays driven by Marangoni convection and thermocapillary effect. Finally, highly ordered porous structure remains on the surface after complete evaporation of the organic solvent and the water droplets. Thus, preparation of porous films in BF process relies on the nucleation and growth of water droplets [25,26], which is susceptible to experiment parameters, such as solvent [27], temperature [28], relative humidity [29], concentration [30], polymer types and architecture [31–34]. Nowadays, there exists the challenge of attempting to optimize conditions for different BF system because of its complexity. On the other hand, manipulation of experimental conditions and polymers will give rise to BF patterns with variable topography and chemical composition for specific applications.

An increasing number of researches are focused on the fluorinated BF patterns [31,32,35–39], since fluorinated polymers possess strong thermal stability, chemical corrosion resistance, low surface energy and low refractive coefficient. Rodríguez-Hernández et al. achieved selective functionalization of the external surface in honeycomb structured porous films with the blends of PS and PS-P5FS [37]. Qiao et al. synthesized a series of poly(PFPA-*ran*-MMA) star fluorinated polymers and investigated the effect of fluorine content on the formation of honeycomb films and physical property of resulting film [32]. Hietala et al. prepared breath figure films from three semifluorinated diblock copolymers to compare their porous morphology and surface properties including wetting behavior and binding capability [31]. These studies indicate that it is feasible to fabricate ordered honeycomb films from fluorinated polymers via breath figure method.

Wetting behavior is measured by contact angle (CA) and can be determined jointly by surface energy and surface roughness according to Wenzel, Cassie, and Baxter [14,40]. Fluorinated polymer films exhibit excellent hydrophobic and oleophobic property due to the surface enrichment of fluorinated units. In terms of a flat film, even the densely packed CF_3, the lowest surface energy chemical group, just has a theoretical CA of 120° [41,42]. For wider application, it is necessary to further enhance hydrophobicity by constructing rough surface, just as super-hydrophobic self-cleaning plant leaves in nature. Generally, honeycomb ordered films fabricated via breath figure have a surface porosity highly more than 50% and controllable pore size, thus it is an ideal candidate to prepare rough structures. Combining with low surface energy of fluorinated polymers and high surface roughness of breath figure arrays, wetting ability of films could be improved in a large extent. Yabu et al. prepared superhydrophobic and oleophobic surfaces from fluorinated polymers via dynamic breath figure. Water contact angle of honeycomb ordered film was 145°, much higher than that of flat film. After peeling off the top-layer, a pincushion structure with CA of 170° was formed [14].

However, detailed investigation on the optimized preparation of fluorinated honeycomb film is still limited in previous reports. Besides, the wetting behavior of fluorinated honeycomb film is expected to be further investigated. In addition, excellent hydrophobicity of the honeycomb films usually comes from relatively high fluorine content, which is not beneficial to the regularity and industrial applications.

In this paper, a series of fluorinated block copolymers with different fluorine content, poly(methyl methacrylate)-*block*-poly(perfluoroalkyl ethyl acrylate) (PMMA-*b*-PFAEA), were used to fabricate honeycomb ordered films via static breath figure method. Effect of temperature, concentration, relative humidity and fluorine content on the morphology of porous films was systemically investigated. In addition, wetting behavior of corresponding flat film, honeycomb film and pincushion-structure film was studied and compared. The wetting property of polymer films was further tailored by changing the PFAEA segment ratio and surface morphology. Moreover, blends of PMMA and PMMA-*b*-PFAEA with variable ratios were applied to fabricate ordered porous films of excellent hydrophobicity and oleophobicity with low fluorine content via simultaneous processes of breath figure and phase separation.

2. Experimental section

2.1. Materials

The fluorinated copolymers of poly(methyl methacrylate)-*block*-poly(perfluoroalkyl ethyl acrylate) (PMMA-*b*-PFAEA) with different fraction of PFAEA were synthesized via reversible addition fragmentation chain transfer (RAFT) method as previously reported [43,44]. Scheme 1 depicts the chemical structure of the fluorinated copolymer. Characteristics of the resulting polymers are listed in Table 1. High molecular-weight poly(methyl methacrylate) (Mn: 5.64×10^5) was used as polymeric matrix in blend system. Water used in all of the experiments was deionized and ultrafiltrated to 18.2 MΩ. All other reagents, purchased from Adamas-beta, were used without further purification.

2.2. Fabrication of copolymer films

Polymers were dissolved in chloroform with concentrations from 1 to 20 mg mL^{-1}. Glass slides were cut into square (0.8 cm^2), ultrasonic cleaned in ethanol for 30 min, and then dried in 50 °C vacuum before usage. Honeycomb films were fabricated in constant temperature and humidity chamber equipped with gloves by casting 20 μL polymer solution onto the glass substrate placed in a glass vessel. With the volatilization of organic solvent, the transparent solution became turbid and honeycomb films were obtained after complete solvent evaporation. The pincushion structure films were prepared by peeling off the top layer of the honeycomb films using adhesive tape. The adhesive tape was stuck firmly to the film surface, and the tape with the adhering top layer was separated from the bottom layer which remained on the substrate. For comparison, flat films were prepared by spin coating on glass substrates for 30 s with a speed of 1000 r/min at room temperature.

2.3. Characterization

Morphologies of the films were characterized by optical microscopy (OM), atomic force microscopy (AFM) and scanning electron

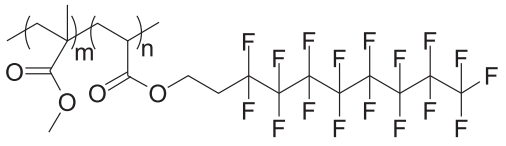

Scheme 1. The chemical structure of PMMA-*b*-PFAEA.

Table 1
Characteristics of PMMA-*b*-PFAEA diblock copolymer.

Sample	M_n (g mol^{-1})[a]	PDI	$M_{n\ PMMA}$[b]	F (wt)[c]
Copolymer 1	1.91×10^4	1.5	1.85×10^4	2.1%
Copolymer 2	8.29×10^4	1.6	8.26×10^4	5.0%
Copolymer 3	1.70×10^4	1.6	1.3×10^4	12.8%
Copolymer 4	2.99×10^4	1.6	1.3×10^4	36.1%

[a] Calculated based on the following equation: $M_{n\ PMMA\text{-}b\text{-}PFAEA} = M_{n\ PMMA} + DP_F \times 554$, DP_F was calculated based on the following equation: $F\% = (DP_F \times 18 \times 19)/(M_{n\ PMMA} + DP_F \times 554)$.
[b] Determined by GPC.
[c] Determined by F-EA.

microscopy (SEM). The morphologies of the films were firstly observed with an optical microscope (Cryo-CSS450) and the images were taken with a digital camera. Elaborate morphologies of the films were obtained by field emission SEM (Hitachi S-4800) at an accelerating voltage of 15.0 kV from samples coated with Au. The sizes of prepared films including pore size and pore-to-pore distance were measured using Nano-measure software. AFM images were obtained with multimode atomic force microscopy (PARK/XE-100) using the noncontact mode under an ambient condition and analyzed by XEI image processing program. Contact angles of distilled water and diiodomethane on the prepared films were measured by pendent drop method using a contact angle analyser (Powereach JC200D3) as follows: a 5 μL liquid droplet was gently placed onto the films, and contact angles were measured by the $\theta/2$ method after 20 s placement. For each angle reported, at least nine sample readings from three surface locations of three different samples were averaged. The surface chemistry analyses of films were completed on an X-ray Photoelectron Spectroscopy (XPS) analyzer (ESCALAB250Xi).

3. Results and discussion

3.1. Fabrication of honeycomb porous films

Honeycomb films were fabricated via static breath figure approach by casting chloroform solution of fluorinated copolymers onto glass slide in a constant temperature and humidity chamber. Representative images of HC films from copolymer 1 are shown in Fig. 1. From the OM image (Fig. 1a), it is found that the pores of films via breath figure are highly regularly arranged in a large area. Due to sunlight diffraction and interference effects on highly ordered films surface, the obtained film exhibits an interesting nacre color as illustrated in the inset of Fig. 1a. Precise morphological observation by SEM (Fig. 1b) and AFM (Fig. 1c) demonstrates that the obtained film consists of highly ordered monolayer structure (inset in Fig. 1b) with hexagonal arrays and uniform size. Based on the SEM and AFM images, the pore size is measured to be ~3.03 μm, while the pore-to-pore distance is 3.63 μm.

BF method enables us to tailor the size, morphology, and regularity of the pores by varying experimental conditions. Herein, we systematically investigated the effects of temperature, concentration, relative humidity and fluorine content of copolymer on morphology of the formed porous films.

The atmosphere temperature in the BF process contributes to solubility, viscosity, evaporation of solvent, segmental motion of polymers and precipitation at the water-solution interface. Fig. 2 shows the influence of atmosphere temperature on the morphology of honeycomb films fabricated from copolymer 1 at a concentration of 10 mg mL^{-1} with 80% relative humidity. The pore size decreases with the increasing of temperature from 30 °C to 50 °C and highly ordered HC film is formed at 50 °C. Increasing temperature results in faster evaporation of solvent and shorter time for the growth of water droplets, which eventually generates smaller pore size of obtained films. Another reason for this phenomenon is that the molecule chain motion becomes easier and the precipitation of copolymers at the water-solution interface becomes faster with increasing temperature. In addition, high temperature leads to good solubility and dispersity of fluorinated copolymers in $CHCl_3$, thus a highly ordered porous film can be formed at 50 °C.

Initial polymer concentration played the other important role in the morphology of the formed porous film. SEM images of porous films of copolymer 1 fabricated at 50 °C under 80% relative humidity with various concentration are illustrated in Fig. 3. Clearly, ordered HC porous films are fabricated in the concentration range from 5 mg mL^{-1} to 20 mg mL^{-1} (Fig. 3b–e) and disordered patterns are observed at 1 mg mL^{-1} (Fig. 3a). The average pore size decreases with the increase of initial polymer concentration. The effect of concentration on the HC films formation is explained as follows. To begin with, concentration determines the viscosity and density of copolymer solution, affecting the immersion depth of condensate water droplets into the solution. Additionally, the growth rate of the droplets is proportional to the temperature difference (ΔT) between the temperature of atmosphere and the temperature of the solution surface, which is described as $dR/dt \sim \Delta T^{0.8}$ [36]. According to the Henry law [45], lower vapor pressure resulting from more concentrated solution induces slower evaporation rate of solvent, which further generates smaller surface temperature gradient (ΔT). Moreover, in terms of certain copolymers, concentration corresponds to the amount of molecular chain, influencing the rate of precipitating at the water-solvent interface and the ability of encapsulating the water droplets. Considering the above-mentioned factors, at the extremely low concentration of 1 mg mL^{-1}, the viscosity is too low and the number of the molecular chains is too few to prevent the water droplets from

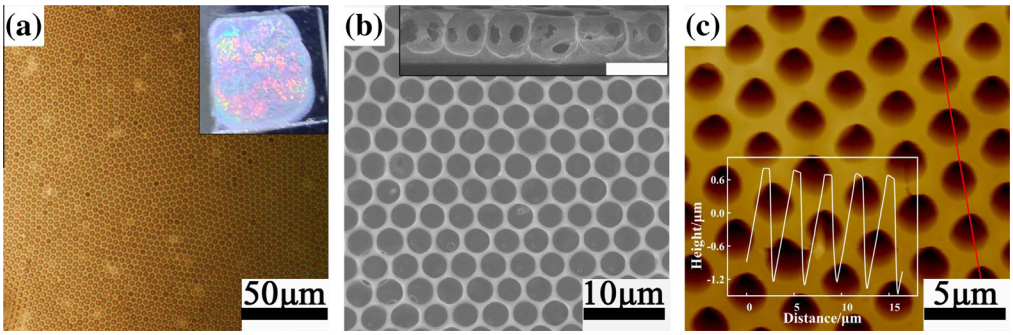

Fig. 1. (a) Optical microscopy image of the porous film fabricated from copolymer 1, inset: photograph of sunlight diffraction. (b) Top view, inset: cross-section view of SEM image, scale bar is 5 μm. (c) AFM topographic image, inset: height profiles of the honeycomb ordered film.

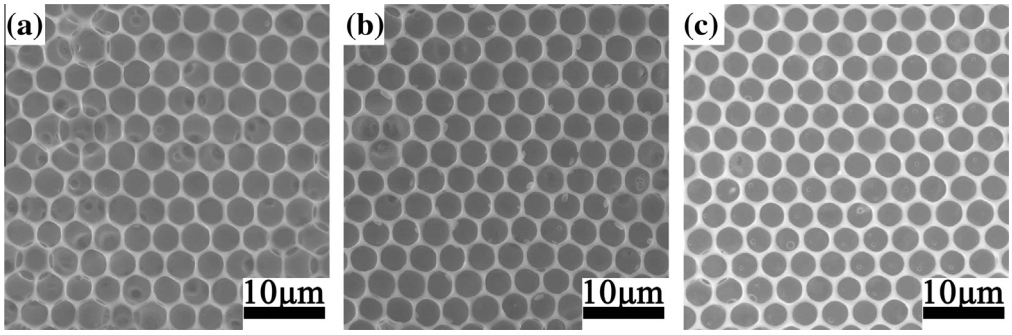

Fig. 2. SEM images of porous films fabricated from copolymer 1 with concentration of 10 mg mL^{-1} under 80% relative humidity at (a) 30 °C, (b) 40 °C, and (c) 50 °C.

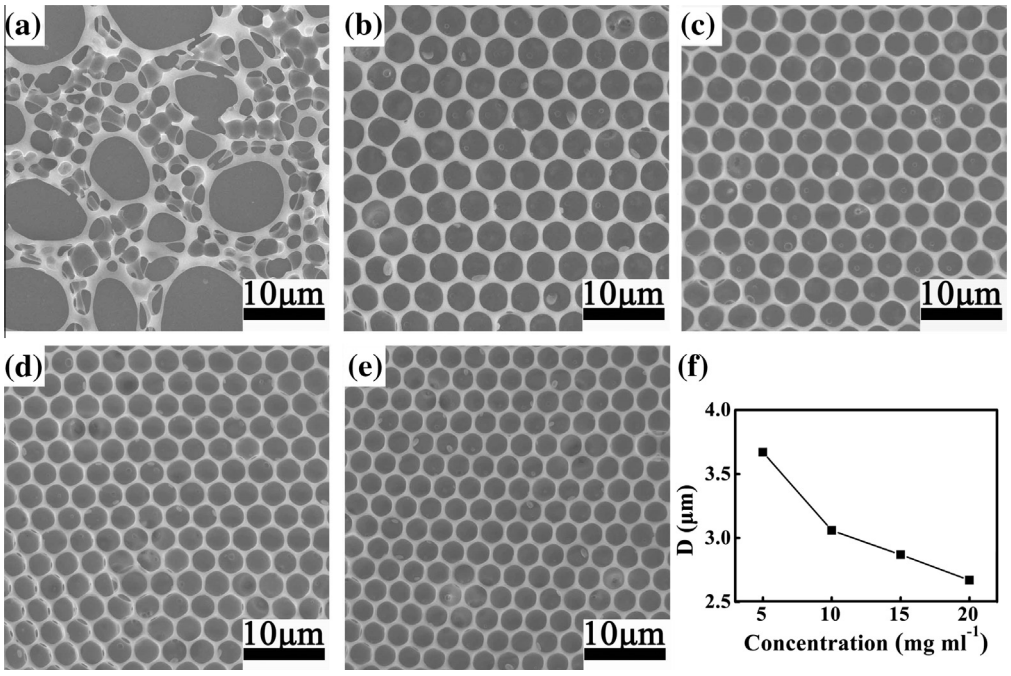

Fig. 3. SEM images of porous films fabricated from copolymer 1 under 80% relative humidity at 50 °C with concentration of (a) 1 mg mL^{-1}, (b) 5 mg mL^{-1}, (c) 10 mg mL^{-1}, (d) 15 mg mL^{-1} and (e) 20 mg mL^{-1}. (f) Dependence of the average pore sizes (D) on the concentration of copolymer.

coalescing, generating larger and irregular pores. Higher concentrated solution leads to tinier water droplets and smaller pore size (Fig. 3f) of resulting films due to the smaller original condensate water droplets and slower growth rate. Therefore, higher concentration ranging from 5 mg mL^{-1} to 20 mg mL^{-1}, is suitable for the fabrication of ordered HC porous films.

Notably, relative humidity is one of the most important factors influencing the morphology of porous films in BF technique. Generally, environment with relative humidity more than 50% is requisite for the condensation of water droplets and formation of porous structures [46]. Fig. 4 exhibits the SEM images of HC porous films fabricated from 10 mg mL^{-1} solutions of copolymer 1 at 50 °C under the relative humidity from 60% to 90%. As shown in Fig. 4a, disordered porous film is formed under 60% humidity. In this case, the atmosphere humidity is so low that the water vapor produces less condensation and the water droplets grow and coalesce irregularly. When the relative humidity ranges from 70% to 90%, highly ordered pores appear on the films surface (Fig. 4b–e) on account of condensation of enough water droplets and their optimal growth. Furthermore, a trend is observed in Fig. 4f that the average pore size increases with the increase of relative humidity. The reasons can be ascribed to the following issues. The growth rate of water droplets is accorded with $dR/dt \sim \varphi_v$, where atmosphere humidity determines φ_v, the flux of vapor molecules per unit area [47]. The growth rate of droplets becomes faster with the increase of the humidity of atmosphere, generating larger pore size. Consequently, it is achievable to obtain porous films of certain pore size by controlling relative humidity in BF fabrication process.

Fig. 5 depicts the SEM images of porous films fabricated from 10 mg mL^{-1} solutions of copolymers with different fluorine content at 50 °C under 80% relative humidity. Although film prepared from copolymer 1 exhibits highly ordered patterns (Fig. 1), copolymers with more fluorine content generate irregular pore structures (Fig. 5). The film surface of copolymer 2 is filled with large pores with size of ~13 μm, existing with much smaller pores (Fig. 5a). Compared to copolymer 1, relative smaller and extremely sparser pores distribute randomly on the surface of copolymer 3 film (Fig. 5b). Fig. 5c shows the irregular pattern with variable pore sizes fabricated from copolymer 4. The formation of disordered porous films is attributed to the weaker ability of more fluorine

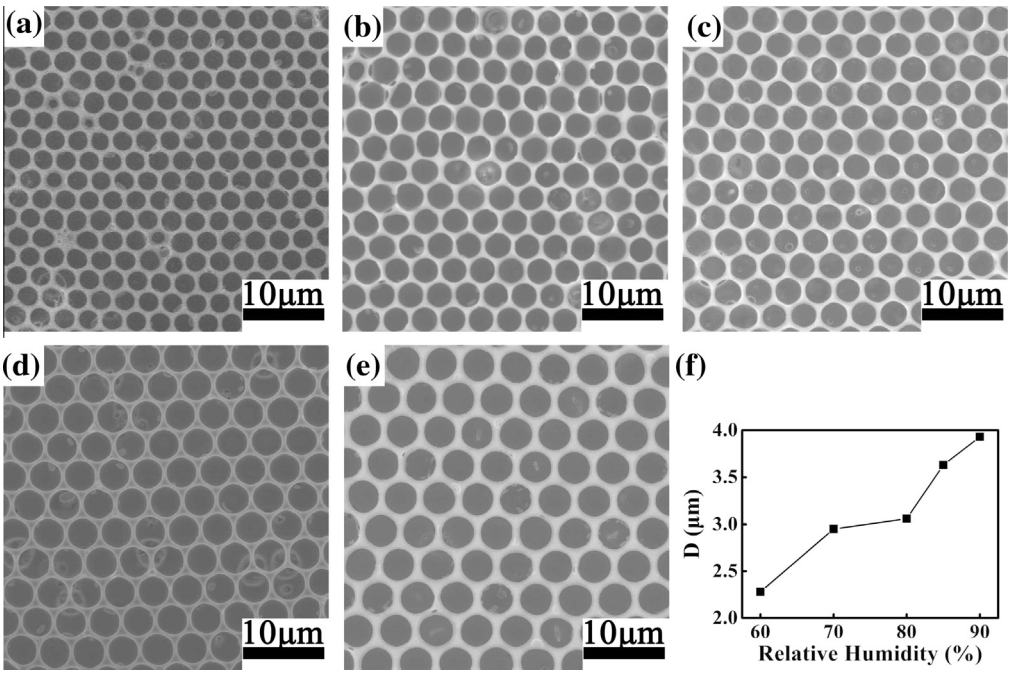

Fig. 4. SEM images of porous films fabricated from copolymer 1 with concentration of 10 mg mL^{-1} at 50 °C under relative humidity of (a) 60%, (b) 70%, (c) 80%, (d) 85%, and (e) 90%. (f) Dependence of the average pore sizes (*D*) on the relative humidity of atmosphere.

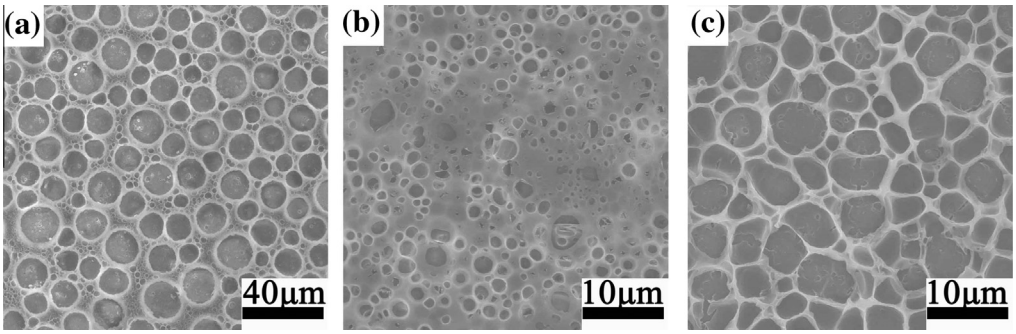

Fig. 5. SEM images of porous films fabricated from various copolymers with concentration of 10 mg mL^{-1} under 80% relative humidity at 50 °C: (a) copolymer 2; (b) copolymer 3; and (c) copolymer 4.

to precipitate at the water-solution interface. Specific explanations for the respective morphology of each copolymer films are required to study further.

3.2. Surface wetting behavior of fluorinated copolymer films

In general, both the surface chemistry and morphology affect wetting behavior, which is characterized by the contact angle on surface. Materials with water-droplets contact angles (CA_{H2O}) more than 90° and 150° are referred to hydrophobic and superhydrophobic materials, respectively [35]. Copolymers composed of fluorinated acrylate possess low surface free energy, hydrophobic and oleophobic properties due to phase separation and enrichment of fluorinated groups on the surface [48].

The SEM and contact angle images of flat film fabricated via spin-coating are illustrated in Fig. 6a. The contact angle of copolymer 1 with only 2.1 wt% fluorine content reaches 95°, meeting the criterion of hydrophobic materials. However, there is still large promotion space for hydrophobic and oleophobic properties by changing surface roughness. Highly ordered porous film via BF is an effective and economic method to improve surface roughness and further enhance the surface wetting ability. As can be seen in Fig. 6b, the CA_{H2O} on the HC porous film fabricated by breath figure is 132°, which is 37° higher than that of corresponding flat film. After peeling off top layer using adhesive tape, CA of the pincushion-like structure is as high as 143° due to thinner pore wall and higher surface roughness (Fig. 6c).

Fig. 6d shows contact angles of H_2O on the surface of flat films via spin coating and HC films via breath figure from copolymer 2 exhibits a CA_{H2O} of 118°, higher than copolymer 1 with a value of 95°, due to higher fluorine content and lower surface free energy. However, the contact angles of copolymer 3 and copolymer 4 do not enhance with the increase of fluorine content. Presumably, 5 wt% fluorine content is enough to reduce the surface free energy to lowest point and the contact angle of flat film almost reaches highest value. Compared to flat films, the contact angles of corresponding honeycomb films of copolymer 2, copolymer 3, and copolymer 4 were improved to 150°, 135° and 153°, respectively, due to the enhancement of surface roughness. For porous film from copolymer 3, sparse and small pores lead to little improvement of surface roughness, which accounts for a slight increase of contact angle.

Additionally, it is noteworthy that there are two types of wetting state on rough film surface, Wenzel and Cassie–Baxter state models. The Wenzel model corresponds to a complete wetting and liquid drop fills up the roughness grooves, while for the

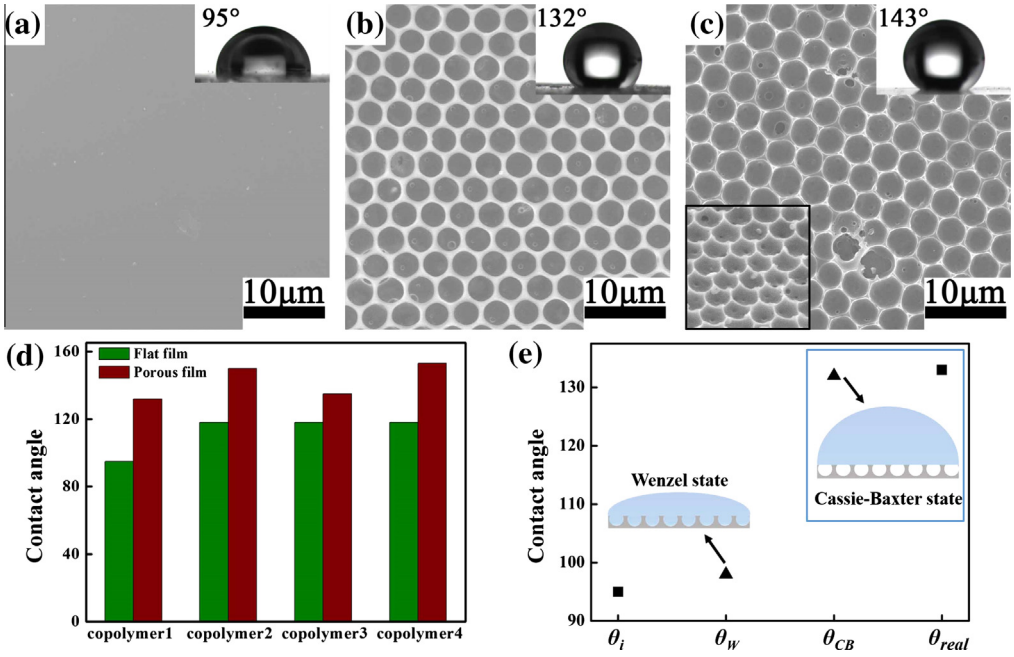

Fig. 6. SEM and contact angle images of (a) flat film via spin coating, (b) honeycomb ordered film via breath figure, and (c) pincushion-like structure via peeling off top layer of (b) from copolymer 1, inset of left bottom: tilted 45 degree view of c. (d) Contact angles of flat films and porous films from different fluorinated copolymers. (e) Contact angles for a flat film (θ_i), a porous film (θ_{real}) of copolymer 1 and predicted values calculated by Cassie–Baxter (θ_{CB}) and Wenzel (θ_W) model.

Cassie–Baxter model, liquid droplets only contacts the top-layer solid and air bubbles trap inside the cavities of the rough film [49]. These two wetting models are described by Eqs. (1) and (2), respectively, where θ is the ideal contact angle on a flat surface, r is the roughness factor defined as the ratio of the actual surface area to the apparent surface area and f is surface area fraction of polymer [50].

$$\cos\theta_W = r\cos\theta_i \quad (1)$$

$$\cos\theta_{CB} = f(\cos\theta_i + 1) - 1 \quad (2)$$

When it comes to the wetting state of honeycomb ordered films via BF technique, either Wenzel model or Cassie–Baxter model can be applied according to different systems [51,52]. For a highly ordered porous film, relations between r and f with pore diameter (D) and pore-to-pore distance (L) are as follows considering hemispherical pores [37]:

$$r = 1 + \frac{\pi D^2}{2\sqrt{3}L^2} \quad (3)$$

$$f = 1 - \frac{\pi D^2}{2\sqrt{3}L^2} \quad (4)$$

In the circumstance of HC film from copolymer 1, the values of obtained r and f are 1.64 and 0.36, respectively. Theoretical contact angles calculated from Wenzel and Cassie–Baxter models are 98.2° and 133°, respectively, while the measured contact angle of HC film is 132°. The results demonstrate that the wetting behavior of HC film in this system is accorded with Cassie-Baxter model, the droplets only wetting the outside surface of pore (Fig. 6e).

3.3. Fabrication and wetting behavior of HC films from blends of copolymer 2 with PMMA

Porous film via BF technique from copolymer 2 is an irregular structure with non-uniform pore size, yet having a contact angle as high as 150° (Fig. 7b). On the contrary, ordered porous film could be obtained from PMMA in specific conditions, with a contact angle of merely 108° (Fig. 7a). Combining respective advantages of above-mentioned two polymer systems by blending, whether a highly ordered film with excellent hydrophobic property could be fabricated is worthy studying.

CA values of HC ordered films from blends of copolymer 2 and PMMA with total concentration of 15 mg mL^{-1} containing different ratio of copolymer 2 from 0 to 15 wt% at 50 °C under 50% RH are shown in Fig. 7c, respectively. On the one hand, the hydrophobic property improves and CA enhances as the blend ratio of copolymer 2 increases. Only 7 wt% ratio of copolymer 2 blending into PMMA, the CA of HC film surface increases from 108° to 143°. No substantial improvement of hydrophobicity is observed for 10 wt % and 15 wt% of copolymer 2 (Fig. 7c). On the other hand, for total concentration of 15 mg mL^{-1}, highly ordered porous films are obtained with the ratio of copolymer 2 under 7% (inset of Fig. 7c). At higher blend ratio of copolymer 2, irregular porous structures with high polydispersities are fabricated due to the weak ability of fluorinated acrylate to stabilize water droplets during BF process. On the basis of above experiments, the optimal blending condition is 7 wt% copolymer 2 in 15 mg mL^{-1} total concentration, from which a regular HC porous film of excellent hydrophobicity is obtained.

Further investigation on the wetting behavior for this specific system is carried out. Water and diiodomethane contact angle on flat films via spin coating and related porous films via BF technique of PMMA, PMMA/PMMA-*b*-PFAEA (14:1) and PMMA-*b*-PFAEA are summarized in Fig. 8. The analysis and comparison of these CA values representing hydrophobicity and oleophobicity are made as follows. Firstly, CA_{H2O} and CA_{CH2I2} of porous films are much higher than that of flat films for above three systems, the reasons of which have been discussed previously. Additionally, no matter for porous films or flat films, hydrophobicity and oleophobicity from blends system with mere 7 wt% fluorinated copolymer 2 are improved significantly when compared to PMMA. This can be ascribed to the fact that the enrichment of fluorine on the film surface leads to low surface energy by phase separation. Image of element composition analysis by SEM–EDS (Fig. 9a) demonstrates the distribution of fluorine and carbon, confirming phase separation of PMMA and PMMA-*b*-PFAEA. Surface free energy can be calculated according to

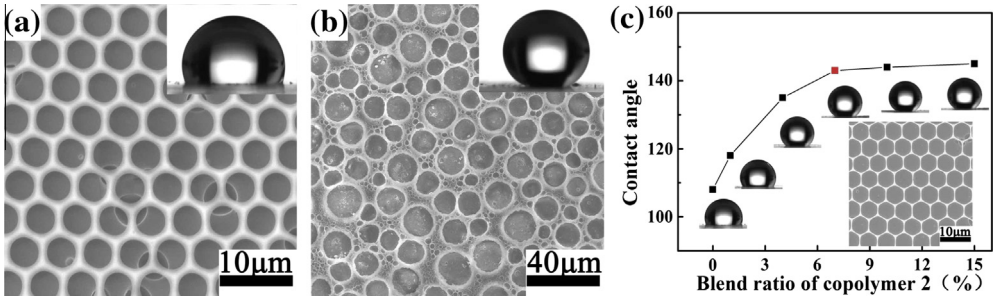

Fig. 7. SEM and CA images of (a) PMMA and (b) copolymer 2. (c) Contact angles of the porous films from the blend of PMMA and PMMA-*b*-PFAEA, inset: SEM image of blend with 7% copolymer 2.

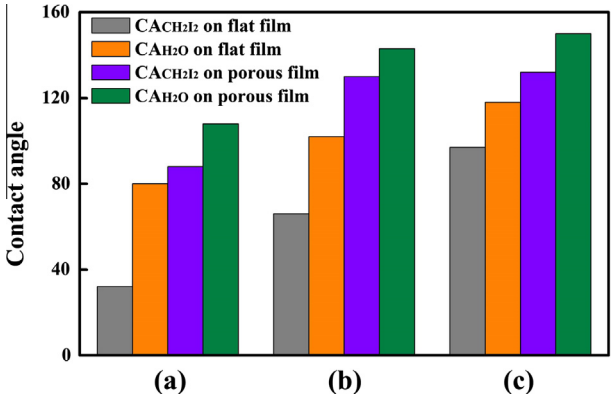

Fig. 8. Water and diiodomethane contact angles on flat films via spin coating and porous films via breath figure from (a) PMMA, (b) blends with 7 wt% of PMMA-*b*-PFAEA, and (c) PMMA-*b*-PFAEA.

following equations, where σ_l^d and σ_l^p represent dispersive and polar contributions of the surface energy for liquid, while σ_s^d and σ_s^p are for solid, respectively [36]. The measuring liquids are water (σ_l^d is 21.8 mN/m and σ_l^p is 51 mN/m) and diiodomethane (σ_s^d is 49.5 mN/m and σ_s^p is 1.3 mN/m). The water and diiodomethane contact angles have been illustrated. Calculated surface free energy of flat films from three polymer systems are listed in Table 2. It is clearly seen that only 7 wt% copolymer 2 could result in extremely low surface free energy of blend system, approaching to copolymer 2.

$$\sigma_1(1+\cos\theta) = 2\left(\sqrt{\sigma_s^d\sigma_l^d} + \sqrt{\sigma_s^p\sigma_l^p}\right) \quad (5)$$

$$\sigma = \sigma^d + \sigma^p \quad (6)$$

Table 2
Surface free energies of three polymer systems.

Solid substrates	σ_s^d (mN m^{-1})	σ_s^p (mN m^{-1})	σ_s (mN m^{-1})
PMMA	44.04	40.8	3.24
PMMA/PMMA-*b*-PFAEA (14:1)	11.48	7.18	4.3
PMMA-*b*-PFAEA	9.88	9.39	0.49

Table 3
Element composition of film from blend as obtained by XPS analysis.

Element	Spin film (%)	HC film (%)	Peel off top layer of HC film (%)
C	64.96	56.67	71.51
O	24.04	19.61	27.13
F	11	23.72	1.36

X-ray photoelectron spectroscopy (XPS) analysis provides further insight into fluorine element on the film surface (Fig. 9b and Table 3). Films prepared from blend system have far more fluorine content than the theoretical ratio, revealing the enrichment of fluorine on the film surface and in accordance with the values of surface free energy. It could be deduced that combined effects of phase separation and BF process make more fluorinated segment migrate to the surface by comparing the fluorine content of spin film and HC film. By peeling off the top layer of HC film, most fluorine disappear, indicating the fluorinated copolymers are located in the top-layer of the outside pore walls (inset of Fig. 9b).

Moreover, when the blend system and PMMA are compared, the increasing extent of hydrophobicity and oleophobicity of HC films is larger than flat films. On the basis of XPS analysis, combined effects of phase separation and BF process make more fluorinated copolymer migrate to the surface. Ordered porous structure as an

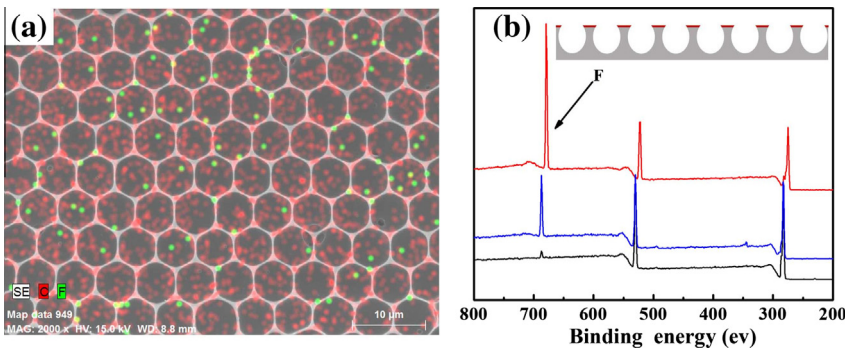

Fig. 9. (a) SEM–EDS image of HC ordered film from blends with 7 wt% of copolymer 2. Red spots represent carbon element, while green spots represent fluorine element. (b) XPS analysis of HC film (red), spin film (blue), peeling off top layer of HC film (black) from blend system, inset: fluorine location of HC film from blends (red regions). (For interpretation of the references to color in this figure legend, the reader is referred to the web version of this article.)

amplifier of wetting ability generates a marked improvement. Therefore it is demonstrated that the low surface energy of copolymer 2 enriching on surface via phase separation and the improvement of surface roughness from HC porous film via BF process jointly determine the remarkable hydrophobicity and oleophobicity of blend system with just 7 wt% copolymer 2.

4. Conclusions

Highly ordered honeycomb porous film has been successfully prepared via breath figure method from PMMA-*b*-PFAEA with 2.1 wt% fluorine content. Preparation conditions including temperature, relative humidity, polymer concentration and fluorine content have been identified as crucial factors for controlling pore size and regularity of the honeycomb porous film. Increase of temperature and polymer concentration results in the decrease of pore size, as well as decrease of relative humidity. Copolymers with higher fluorine content generate irregular porous structure. The obtained films exhibit excellent hydrophobicity due to low surface energy of fluorinated copolymer and high surface roughness of honeycomb porous structure. Moreover, highly ordered film with excellent hydrophobicity and oleophobicity is fabricated from the blends of PMMA and mere 7 wt% of copolymer 2 via combined action of breath figure and phase separation. From the perspective of PMMA, the hydrophobicity of film from blends of polymers has been improved. In terms of PMMA-*b*-PFAEA, the problem of irregular porous pattern from high fluorine content has been settled by this simple and economical method. Meanwhile, it is an effective way to reduce the fluorine fraction and save material cost in preparing films with excellent hydrophobicity and oleophobicity.

Acknowledgements

This work was supported by National Natural Science Foundation of China (51573046 and 51103044). Support from Projects of Shanghai Municipality (14SG29) and Fundamental Research Funds for the Central Universities (NCET-12-0857, B14018 and WD1213002) is also appreciated.

References

[1] A.S. De León, T. Garnier, L. Jierry, F. Boulmedais, A. Muñoz-Bonilla, J. Rodríguez-Hernández, ACS Appl. Mater. Interfaces 7 (2015) 12210.
[2] P.T. Tanev, M. Chibwe, T.J. Pinnavaia, Nature 368 (1994) 321.
[3] S.W. Choi, J. Xie, Y. Xia, Adv. Mater. 21 (2009) 2997.
[4] X. Wu, S. Wang, ACS Appl. Mater. Interfaces 4 (2012) 4966.
[5] A. Martínez-Gómez, C. Alvarez, J. de Abajo, A. del Campo, A.L. Cortajarena, J. Rodriguez-Hernandez, ACS Appl. Mater. Interfaces 7 (2015) 9716.
[6] J. Kim, N. Singh, L.A. Lyon, Angew. Chem. Int. Ed. 45 (2006) 1446.
[7] M. Müller, R. Zentel, T. Maka, S.G. Romanov, C.M. Sotomayor, Torres, Adv. Mater. 12 (2000) 1499.
[8] L. Wan, J. Li, B. Ke, Z. Xu, J. Am. Chem. Soc. 134 (2012) 95.
[9] H. Cong, J. Wang, B. Yu, J. Tang, Soft Matter 8 (2012) 8835.
[10] X. Li, L. Zhang, Y. Wang, X. Yang, N. Zhao, X. Zhang, J. Xu, J. Am. Chem. Soc. 133 (2011) 3736.
[11] L. Li, Y. Zhong, C. Ma, J. Li, C. Chen, A. Zhang, D. Tang, S. Xie, Z. Ma, Chem. Mater. 21 (2009) 4977.
[12] Y. Zhu, R. Sheng, T. Luo, H. Li, J. Sun, S. Chen, W. Sun, A. Cao, ACS Appl. Mater. Interfaces 3 (2011) 2487.
[13] W.-H. Ting, C.-C. Chen, S.A. Dai, S.-Y. Suen, I.K. Yang, Y.-L. Liu, F.M.C. Chen, R.-J. Jeng, J. Mater. Chem. 19 (2009) 4819.
[14] H. Yabu, M. Takebayashi, M. Tanaka, M. Shimomura, Langmuir 21 (2005) 3235.
[15] A. Muñoz-Bonilla, M. Fernández-García, J. Rodríguez-Hernández, Prog. Polym. Sci. 39 (2014) 510.
[16] Q. Liu, Z. Tang, B. Ou, L. Liu, Z. Zhou, S. Shen, Y. Duan, Mater. Chem. Phys. 144 (2014) 213.
[17] D. Wu, F. Xu, B. Sun, R. Fu, H. He, K. Matyjaszewski, Chem. Rev. 112 (2012) 3959.
[18] W. Wang, C. Du, X. Wang, X. He, J. Lin, L. Li, S. Lin, Angew. Chem. Int. Ed. 53 (2014) 12116.
[19] M. Behl, J. Seekamp, S. Zankovych, C.M. Sotomayor Torres, R. Zentel, J. Ahopelto Adv. Mater. 14 (2002) 588.
[20] L. Guangming, W.B. Larry, Nanotechnology 18 (2007) 245302.
[21] Y. Lei, S. Yang, M. Wu, G. Wilde, Chem. Soc. Rev. 40 (2011) 1247.
[22] R.N. Leach, F. Stevens, S.C. Langford, J.T. Dickinson, Langmuir 22 (2006) 8864.
[23] S. Anand, K. Rykaczewski, S.B. Subramanyam, D. Beysens, K.K. Varanasi, Soft Matter 11 (2015) 69.
[24] A. Zhang, H. Bai, L. Li, Chem. Rev. 115 (2015) 9801.
[25] H. Bai, C. Du, A. Zhang, L. Li, Angew. Chem. Int. Ed. 52 (2013) 12240.
[26] L. Wan, L. Zhu, Y. Ou, Z. Xu, Chem. Commun. 50 (2014) 4024.
[27] E. Ferrari, P. Fabbri, F. Pilati, Langmuir 27 (2011) 1874.
[28] H. Yabu, M. Tanaka, K. Ijiro, M. Shimomura, Langmuir 19 (2003) 6297.
[29] R. Zhang, J. Wang, M. Wang, Y. He, J. Appl. Polym. Sci. 124 (2012) 495.
[30] Y. Tian, S. Liu, H. Ding, L. Wang, B. Liu, Y. Shi, Macromol. Chem. Phys. 207 (2006) 1998.
[31] L. Valtola, M. Karesoja, H. Tenhu, P. Ihalainen, J. Sarfraz, J. Peltonen, M. Malinen, A. Urtti, S. Hietala, J. Appl. Polym. Sci. 132 (2015) 41125.
[32] Z. Zhang, T.C. Hughes, P.A. Gurr, A. Blencowe, H. Uddin, X. Hao, G.G. Qiao, Polymer 54 (2013) 4446.
[33] L.A. Connal, R. Vestberg, C.J. Hawker, G.G. Qiao, Adv. Funct. Mater. 18 (2008) 3706.
[34] L.A. Connal, P.A. Gurr, G.G. Qiao, D.H. Solomon, J. Mater. Chem. 15 (2005) 1286.
[35] Y. Xue, H. Lu, Q. Zhao, J. Huang, S. Xu, S. Cao, Z. Ma, Polym. Chem. 4 (2013) 307.
[36] Z. Li, X. Ma, D. Zang, B. Shang, X. Qiang, Q. Hong, X. Guan, RSC Adv. 4 (2014) 49655.
[37] A.S. de Leon, A.d. Campo, C. Labrugere, M. Fernandez-Garcia, A. Munoz-Bonilla, J. Rodriguez-Hernandez, Polym. Chem. 4 (2013) 4024.
[38] A.S. de León, A. del Campo, M. Fernández-García, J. Rodríguez-Hernández, A. Muñoz-Bonilla, A.C.S. Appl, Mater. Interfaces 5 (2013) 3943.
[39] S. Qin, H. Li, W. Yuan, Y. Zhang, J. Mater. Sci. 47 (2012) 6862.
[40] N.E. Zander, J.A. Orlicki, A.S. Karikari, T.E. Long, A.M. Rawlett, Chem. Mater. 19 (2007) 6145.
[41] A. Otten, S. Herminghaus, Langmuir 20 (2004) 2405.
[42] A. Hozumi, O. Takai, Thin Solid Films 303 (1997) 222.
[43] Y. Wei, X. Li, K. Wang, W. He, Z. Han, Acta Chim. Sin. 66 (2008) 1470.
[44] X. Li, Y. Yang, G. Li, S. Lin, Polym. Chem. 5 (2014) 4553.
[45] Y. Xu, B. Zhu, Y. Xu, Polymer 46 (2005) 713.
[46] M. Hernandez-Guerrero, M.H. Stenzel, Polym. Chem. 3 (2012) 563.
[47] B. Zhao, J. Zhang, H. Wu, X. Wang, C. Li, Thin Solid Films 515 (2007) 3629.
[48] N.M.L. Hansen, M. Gerstenberg, D.M. Haddleton, S. Hvilsted, J. Polym. Sci., Part A: Polym. Chem. 46 (2008) 8097.
[49] Y.Y. Yan, N. Gao, W. Barthlott, Adv. Colloid Interface Sci. 169 (2011) 80.
[50] H. Yabu, Y. Hirai, M. Kojima, M. Shimomura, Chem. Mater. 21 (2009) 1787.
[51] B. Ke, L. Wan, Y. Li, M. Xu, Z. Xu, PCCP 13 (2011) 4881.
[52] E. Min, K.H. Wong, M.H. Stenzel, Adv. Mater. 20 (2008) 3550.